Lattice Boltzmann Simulation of Mixed Convection Around a Heated Elliptic Block Cylinder within a Lid-driven Square Cavity

ABDELHAK DAIZ[1,*], AHMED BAHLAOUI[1], ISMAIL ARROUB[1], SOUFIANE BELHOUIDEG[1], ABDELGHANI RAJI[2], MOHAMMED HASNAOUI[3]
[1]Research Laboratory in Physics and Sciences for Engineers (LRPSI),
Polydisciplinary Faculty,
Béni-Mellal,
MOROCCO

[2]Energy and Materials Engineering Laboratory (LGEM),
Faculty of Sciences and Technics,
Béni-Mellal,
MOROCCO

[3]Laboratory of Fluid Mechanics and Energetics (LMFE),
Faculty of Sciences Semlalia, Marrakech,
MOROCCO

**Corresponding Author*

Abstract: - A numerical analysis of mixed convection flows and heat transfer in a square enclosure having a sliding wall containing an elliptical block heated by isothermal temperature has been carried out. The enclosure is full of air and cooling from its sides by a cold temperature, whereas the remaining walls of the enclosure are considered thermally insulated. The mixed convection impact is attained by the heating elliptic block and moving upper wall. The investigation of fluid's hydrodynamic and thermal behavior was examined by using Lattice Boltzmann Method (LBM) at different locations and orientations of the interior elliptical block for Richardson number, Ri, varying from 0.01 to 100 while the Rayleigh number, Ra, is fixed at 10^4. The findings indicate that the temperature pattern and flow structure are very responsive to the position of the elliptical block and Richardson number. Also, it is found that the heat exchange is very important for the block placed vertically close to the left wall or horizontally close to the bottom wall. More precisely, for Ri = 0.01, by moving the vertical block from the center towards the vicinity of the left/ (the right) surface, the heat transfer rate increases from 5.44 to 11.06/(8.36) with an increase of 103.30%/(53.67%). On the other hand, it is noted that the horizontal elliptic block favors heat evacuation in comparison with the vertical one. This study's real-world impact lies in the potential to improve our understanding and, consequently, design more efficient cooling systems for electronic devices.

Key-Words: - Numerical analysis, Mixed convection, Lid-driven cavity, Elliptic block, Lattice Boltzmann method, Block locations, Block orientations, Heat evacuation.

Received: April 15, 2023. Revised: September 21, 2023. Accepted: November 17, 2023. Published: December 31, 2023.

1 Introduction

Mixed convection heat transfer has always attracted a lot of attention due to its wide applications in various fields such as cooling of electronic equipment [1], [2], solar energy collectors [3], chemical processing equipment [4], [5], and heat exchangers [6], [7]. The combined free and forced convection problems are mostly linked to the ventilated and lid-driven enclosures [8], [9], [10], [11], [12].

Over the years, many authors have devoted their attention to studying the characteristics of convection flow and heat transfer with blocks. Several studies have considered free convection in cavities containing blocks with different boundary conditions. In this context, several studies carried out free convection inside a cold square enclosure

with a variety of shaped inner blocks [13], [14]. Their findings demonstrated that the maximum heat exchange is observed at the ellipse's orientation 30° and Ra = 10^6. They discovered that when aspect ratio and Ra were taken into range consideration, the heat exchange rises by augmenting aspect ratio (AR) and Ra. Furthermore, with the exception of AR = 0.1, it is observed that the inclination of the rectangular obstruction often increased the heat exchange rate. It has been demonstrated that the mean Nusselt number goes up as the Ra increases, and its lowest value moves further away from the upper wall of the inner cylinder. In other studies, [15], [16], [17] have analyzed natural convection with blocks in a cold vertical-sided square cavity. It is observed that for low Ra, the inclination angle had no appreciable influence on the typical Nusselt number. The size of the central obstruction has a significant impact on the mean Nusselt number, and it reduces considerably as the diameter of the interior block grows. Also, the increase in block size has enhanced heat exchange caused by increasing the lower block surface. [18], [19] studied the influence of various sizes and positions of the heating cylinder block in a square enclosure. The obtained outcomes demonstrate that the mean Nusselt number, Nu, diminishes with the growth of the block size. Also, they conclude that an increase in the Nu for all positions of the block and the lack of the effect of magnetic field (Ha = 0), whereas augmenting the Hartmann number lowered the mean Nusselt number.

Several studies dealing with forced convection have considered channels with blocks inside, [20], [21] have numerically explored the forced convection in a rectangular channel containing heated square blocks. They obtained that because of the asymmetric fluid flow, the local Nusselt number evaluated on the upper and bottom walls is not identical to the heat exchange that a unique obstruction suffers. The mean Nusselt number rises by increasing Re. Beyond critical Re, the Nusselt number calculated on the lower wall is larger than that calculated on the upper wall. The results reveal that adding a flat plate with a height of h = 2D in front of the cylinder block increases the heat exchange through heated cylinders to enter the fluid. The altering effect of fin size on heat exchange and cooling liquid flow behavior in the channel was numerically investigated by [22]. The author observed that heat sinks with a fin size of 0.8 mm have significant heat transfer, which is greater compared to 0.9 mm and 1.0 mm fin sizes (Totally enclosed thermal dissipator). [23] experimentally examined the forced convection in a horizontal duct containing a set of aluminum blocks. At this point, the block's temperature drops by increasing the Reynolds number while the mean Nusselt number increases. For small Reynolds numbers, when the convective coefficient of heat transfer decreases, the block's temperature rises. Recently, [24] performed an analysis of forced convection characteristics in a horizontal duct with triple hot obstructions by applying Lattice Boltzmann Method (LBM-MRT). It is observed that raising the thermal conductivity of the solid fluid improves the heat exchange. In addition, as the spacing between obstructions increases, the heat exchange for second and third obstructions increases. Also, the use of many jets in the analyzed array improves heat transfer.

Combined natural and forced convection is frequently observed in very high-output appliances when forced convection or free convection is insufficient to remove all necessary heat. At this stage, great attention has been dedicated to the possibility of increasing the heat exchange by mixed convection in rectangular cavities by the presence of various block shapes. In this regard, [25] explored a computational investigation of the laminar flow mixed convection in a vented enclosure containing a hot square block situated in the enclosure center. The findings demonstrate that as the Re and Ri rise, so does the mean Nusselt number around the heating interior block. They also found that the influence of the positions and size (aspect ratio) of the interior block has an important role in the flow and temperature patterns. Further studies on the insertion of blocks inside of the cavity [26], [27]. They concluded that the heat exchange rate calculated on the heated surface of the cavity rises for low values of Ri and reduces for greater values of Ri and by increasing cylinder diameter in both situations of vertical wall or lower wall heated. Moreover, the rate of heat transmission increases as block diameter and heat generation rise, whereas it decreases when the thermal conductivity ratio rises. The upsurge of the block diameter, thermal conductivity ratio, and heat generating characteristics cause the fluid's average temperature to rise. For such configurations, [28] numerically examined mixed convection of laminar flow in a lid-driven square enclosure having a square hot obstacle inside. The authors noticed that the most optimal heat exchange achieved for the blocking is located in the top left and lower right-hand angles of the enclosure. [29] numerically studied the mixed convection heat transfer in a lid-driven square cavity containing a circular block inside. Their derived results demonstrate that the existence of the circular block entails an augmentation of the mean Nusselt

number compared with the absence of a circular block. Also, the mean Nusselt number grows by growing the cylinder block diameter for different Ri. The same work has been done by, [30]. It is noticed that the current lines and the isotherms within the enclosure are highly dependent on the locations of the circular block and the relative of the convection dominates regime (natural, forced, or mixed). [31], studied the impact of thermally insulated obstruction in an enclosure with moving vertical walls and differential heating on mixed convection. The findings show that the thermal exchange inside the cavity improves up to a specific block size. Recently, [32], explored the effect of the triangle obstruction position with uniform thermal flux on the vertical median of the square enclosure with a moving wall. The outcomes of this investigation indicate a great heat exchange rate in the case of the block located at the cavity center. Also, the Nusselt number declines with increasing Ri.

According to the aforementioned review of literature, a computational examination of combined free and forced convection from an obstacle in the shape of an elliptical block enclosed in a square cavity has never been done. The principal goal of the current study is to investigate the influence of position and orientation of heated elliptical obstruction on mixed convection in a square moving wall enclosure. The side surfaces are maintained at cold temperatures whereas the remaining surfaces of the enclosure are adiabatic. The upper wall is moving at a uniform speed. The flow-controlling parameters employed in this study are the Richardson number (Ri), position, and orientation of the elliptical cylinder.

2 Problem Formulation

2.1 Problem Statement

The schematic representation of the studied configuration is illustrated in Figure 1. It consists of a lid-driven square enclosure, containing a heated elliptical block by a hot temperature. The size of the elliptical block is 0.2 and 0.1 on semi-major axis and semi-minor, respectively. The horizontal walls of the enclosure are kept thermally insulated while the side walls are subjected to cold temperatures. The air, as the working fluid in this work, is considered Newtonian, incompressible, and circulating in a laminar regime. All air thermophysical characteristics are supposed to be made unchanged, apart from the density in the floatability expression. The latter (density) is evaluated using the Boussinesq model.

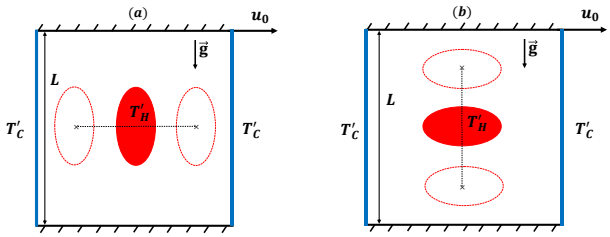

Fig. 1: Diagram of the studied configuration

2.2 Governing Equations

Based on the preceding hypothesis, the continuity, momentum, and energy equations, obtained by the application the conservation of mass, momentum, and energy, in a two-dimensional Cartesian coordinate system in dimensionless forms are as listed below:

$$\frac{\partial U}{\partial X}+\frac{\partial V}{\partial Y}=0 \tag{1}$$

$$\frac{\partial U}{\partial t}+U\frac{\partial U}{\partial X}+V\frac{\partial U}{\partial Y}=-\frac{\partial P}{\partial X}+\frac{1}{Re}\left(\frac{\partial^2 U}{\partial X^2}+\frac{\partial^2 U}{\partial Y^2}\right) \tag{2}$$

$$\frac{\partial V}{\partial t}+U\frac{\partial V}{\partial X}+V\frac{\partial V}{\partial Y}=-\frac{\partial P}{\partial Y}+\frac{1}{Re}\left(\frac{\partial^2 V}{\partial X^2}+\frac{\partial^2 V}{\partial Y^2}\right)+Ri.T \tag{3}$$

$$\frac{\partial T}{\partial t}+U\frac{\partial T}{\partial X}+V\frac{\partial T}{\partial Y}=\frac{1}{RePr}\left(\frac{\partial^2 T}{\partial X^2}+\frac{\partial^2 T}{\partial Y^2}\right) \tag{4}$$

Where $Re=u_0L/\vartheta$, $Ri=Ra/(PrRe^2)$, $Ra=g\beta\Delta T'L^3/\alpha\vartheta$ and $Pr=\vartheta/\alpha$ are the Reynolds, Richardson, Grashof and the Prandtl numbers, respectively, and $\Delta T'=T'_H-T'_C$ is the temperature difference, [33].

The foregoing equations are rendered dimensionless by employing the appropriate set of the next dimensionless variables, [34]:

$$\begin{cases}(X,Y)=(x/L,y/L)\,; \quad (U,V)=(u/u_0,v/u_0)\\ t=\dfrac{u_0}{L}t'; \quad P=\dfrac{p}{\rho {u_0}^2}; \quad T=\dfrac{T'-T'_C}{T'_H-T'_C}\end{cases}$$

The limit conditions considered in form of non-dimensional variables are as follows:

$$\begin{cases}U=1,\ V=0 & \dfrac{\partial T}{\partial Y}=0 & at\ \ Y=1\\ V=V=0, & \dfrac{\partial T}{\partial Y}=0 & at\ \ Y=0\\ U=V=0, & T=0 & at\ \ X=0\\ U=V=0, & T=0 & at\ \ X=1\\ U=V=0, & T=1 & in\ the\ block\end{cases}$$

2.3 Numerical Method

The Lattice Boltzmann Model (LBM) is a robust method, that has been widely applied to analyze fluid dynamics in both simple and complex geometries. The reason for the increase in use of this technique is due to the high adaptability in approaching various types of models and the great ease it offers in the implementation and processing of boundary conditions, [35]. This method considers the fluid as a set of particles that move in a uniform network from one node to neighboring nodes during the time interval. In this method, the dynamic and thermal fields are solved by employing two different distribution functions f and g. The discretization of the fluid field into homogeneous sized rectangular cells. A unit cell contains a certain number of functions of distribution that indicate the possibilities for a particle situated in the central node to move in one of the directions determined by the discretization model chosen. For two-dimensional problems, the D2Q9 scheme, illustrated in Figure 2 is the most widespread, and it is the one we have retained in our work for the dynamic and thermal distribution functions. The BGK (Bhatnagar-Gross-Krook) approximation is a simplification used in lattice Boltzmann methods (LBM). Named after its inventors, Bhatnagar, Gross, and Krook, the BGK approximation simplifies the collision operator in the Boltzmann equation, making the computations more tractable, [36].

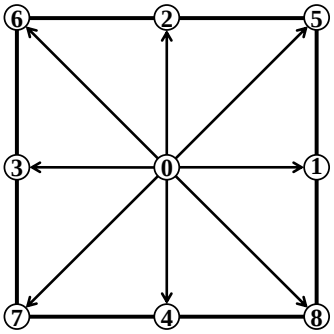

Fig. 2: Schematic diagram of D2Q9 model of lattices discretization.

The governing equations for two distribution functions using the Bhatnagar-Gross-Krook (BGK) approximation can be written as follows, [37]:

$$f_k(r + c_k\Delta t, t + \Delta t) = f_k(r,t) - \frac{1}{\tau_f}\left(f_k(r,t) - f_k^{eq}(r,t)\right) + F_k\Delta t \quad (5)$$

$$g_k(r + c_k\Delta t, t + \Delta t) = g_k(r,t) - \frac{1}{\tau_g}\left(g_k(r,t) - g_k^{eq}(r,t)\right) \quad (6)$$

In the foregoing equations, τ_f and τ_g are the relaxation times for energy and momentum equations, respectively. Also, c_k is the lattice speed in direction k, which is defined below:

$$\vec{c}_k = (c_{kx}, c_{ky}) = c\begin{cases} (0,0)k = 0 \\ (\pm 1,0)k = 1,3 \\ (0,\pm 1)k = 2,4 \\ (\pm 1,\pm 1) \quad k = 5-8 \end{cases} \quad (7)$$

Where c is the lattice speed expressed in equation below:

$$c = \frac{\Delta x}{\Delta t'} = \frac{\Delta y}{\Delta t'} \quad (8)$$

The Δt', Δx and Δy parameters represent the time step, space step in x and y direction, respectively.

In equation (5), F_k, is the external force, its expression is given by, [38]:

$$F_k = 3\omega_k \rho g \beta c_{ky}(T - T_m) \quad (9)$$

With β is the coefficient of the thermal expansion, $T_m = (T_H + T_C)/2$ is non-dimensional reference temperature and ω_k is the weighting parameter given by equation (10):

$$\omega_k = \begin{cases} 4/9 & k = 0 \\ 1/9 & k = 1,\ldots,4 \\ 1/36 & k = 5,\ldots,8 \end{cases} \quad (10)$$

f_k^{eq} and g_k^{eq} are the local equilibrium functions of the dynamic and thermal fields. They are given in the following equations:

$$f_k^{eq}(r,t) = \omega_k \rho \left[1 + \frac{\vec{c}_k.\vec{u}}{c_s^2} + \frac{1}{2}\frac{(\vec{c}_k.\vec{u})^2}{c_s^4} - \frac{1}{2}\frac{\vec{u}.\vec{u}}{c_s^2}\right] \quad (11)$$

$$g_k^{eq}(r,t) = \omega_k T \left[1 + \frac{\vec{c}_k.\vec{u}}{c_s^2}\right] \quad (12)$$

c_s is the speed of sound in the lattice, which equals to $1/\sqrt{3}$ in the D2Q9 model.

The lattice kinetic viscosity and lattice thermal diffusivity are related to the Relaxation times of momentum and energy by the following expressions

$\nu = c_s^2(\tau_f - 0.5)$ and $\alpha = c_s^2(\tau_g - 0.5)$, respectively.

The value of Mach number for the present investigation was Ma = 0.1, which is below the threshold of 0.3 in order not to break the fluid's incompressibility assumption [9]. Lattice viscosity can be determined as a relation of Prandtl number, Mach number and Rayleigh number by using equation (13):

$$\nu = Ma.M\sqrt{\frac{Pr}{3Ra}} \tag{13}$$

With M is the number of knots in the y axis.

All distribution functions in the LBM are defined by collision and streaming steps, although establishing boundary conditions is required before computing the distribution functions. The boundary conditions in the LBM are considerably changed since all not defined steering functions at every limit are necessary to be determined.

The classic rebound technique is used on fixed walls to calculate the unidentified distribution functions, which stream from outside to inside the fluid domain. These unidentified functions are set to their inverse, [39].

$$\begin{cases} f_1 = f_3, f_5 = f_7, f_8 = f_6 \quad (left\ wall) \\ f_2 = f_4, f_5 = f_7, f_6 = f_8 \quad (bottomwall) \\ f_3 = f_1, f_7 = f_5, f_6 = f_8 \quad (rightwall) \end{cases} \tag{14}$$

The longitudinal component of speed on the upper mobile boundary, fluid density, and particle distribution functions are all calculated in equation (15) as follows:

$$\begin{cases} u = u_0 \\ \rho = f_0 + f_1 + f_3 + 2(f_2 + f_5 + f_6) \\ f_4 = f_2 \\ f_7 = f_5 + \frac{1}{2}(f_1 - f_3) - \frac{1}{2}\rho u_0 \\ f_8 = f_6 - \frac{1}{2}(f_1 - f_3) + \frac{1}{2}\rho u_0 \end{cases} \tag{15}$$

Now, let's talk about the boundary conditions of temperature.

For thermally insulated upper and lower walls:

$$\begin{cases} g_{k,0} = \frac{4g_{k,1} - g_{k,2}}{3} \quad k = 0, \dots, 8 \\ g_{k,M} = \frac{4g_{k,M-1} - g_{k,M-2}}{3} \quad k = 0, \dots, 8 \end{cases} \tag{16}$$

For the cold left wall:

$$\begin{cases} g_1 = Tc.(\omega_1 - \omega_3) - g_3 \\ g_5 = Tc.(\omega_5 - \omega_7) - g_7 \\ g_8 = Tc.(\omega_8 - \omega_6) - g_6 \end{cases} \tag{17}$$

For the cold right wall:

$$\begin{cases} g_3 = Tc.(\omega_3 - \omega_1) - g_1 \\ g_6 = Tc.(\omega_6 - \omega_8) - g_8 \\ g_7 = Tc.(\omega_7 - \omega_5) - g_5 \end{cases} \tag{18}$$

The method proposed in, [14], [40], has been utilized for the treatment of the velocity and temperature of the ellipse's curved boundaries.

The macroscopic variables that are the density, ρ, the component velocity, u, v, and the temperature, T, where calculated by the below expressions:

$$\rho = \sum_{K=0}^{8} f_k \tag{19}$$

$$\rho u = \sum_{k=0}^{8} c_{k,y} f_k \tag{20}$$

$$\rho v = \sum_{k=0}^{8} c_k f_k \tag{21}$$

$$T = \sum_{k=0}^{8} g_k \tag{22}$$

2.3 Heat Transfer

The local and mean Nusselt numbers characterizing the heat transfer rate on vertical cold walls are given by the expressions below:

$$Nu = \left| \left(\frac{\partial T}{\partial X}\right)_{X=0,1} \right| \tag{23}$$

$$\overline{Nu} = \int_0^1 Nu\, dY|_{X=0} + \int_0^1 Nu\, dY|_{X=1} \tag{24}$$

3 Independent Grid and Numerical Validation

Preliminary tests were also carried out to check the sensibility of the results to the mesh. The results presented in Table 1 in terms of average Nusselt number for horizontal heated elliptic cylinder block at (0.5;0.5) and for Ra = 10^4 show that a grid of 141×141 (used in the simulation part) is sufficient to describe the flow characteristics because it provides a good balance between the computation time and the required accuracy. More precisely, the refinement of the used grid to 161×161 implies maximum variations less than 0.2 % in terms of $\overline{Nu}$. The calculations were made using the Windows operating system with Intel core i5 of frequency 2.60 GHz and 4 GB of RAM. By analyzing the impact of the grid on CPU time, we found that the refining grid from 141x141 to 161x161 involves a maximum increase of about 48% in computational effort.

Table 1. Grid's effect on average Nusselt number for $Ra = 10^4$ and various Richardson numbers

Grids	101×101	121×121	141×141	161×161
$Ri = 0.1$	6.38	6.43	6.45	6.46
$Ri = 5$	4.90	4.94	4.96	4.97

We limit ourselves here to presenting quantitative and qualitative comparisons between our results and those found by, [29], in the case of mixed convection in a square enclosure with a moving wall whose side surfaces are thermally insulated, the lower surface is kept at a hot temperature and the upper one is kept at a cold temperature and moves to right by uniform speed. An inner cold circular block placed in the center is used for different Richardson numbers Ri by varying Ra at fixed Re = 100 and Pr = 0.7. Figure 3 demonstrates that the streamlines and isotherms generated by, [29], are properly replicated by our numerical code. The comparative quantitative results, reported in Table 2 in the form of average Nusselt numbers assessed on the hot surface, demonstrate a high concordance with maximal differences within 0.55 %.

Table 2. Comparative results of the mean Nusselt number assessed on the hot surface for Re = 100, $r_0/L = 0.2$ and Pr = 0.7

Ri	Present study	Ref. [29]	Max deviations
$Ri = 0.01$	2.904	2.92	0.55%
$Ri = 1$	3.497	3.50	0.086%
$Ri = 5$	4.689	4.96	0.02%
$Ri = 10$	5.045	5.04	0.09%

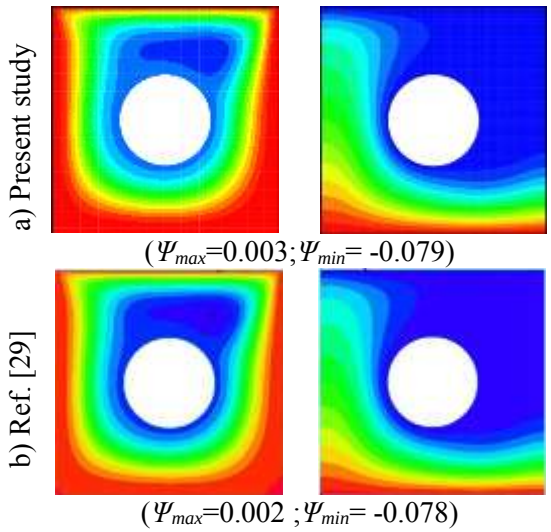

Fig. 3: Comparison in terms of the streamlines and isotherms for $r_0/L = 0.2$, Re = 100 and Ri = 1: a) our results and b) Ref. [29].

4 Results and Discussion

The present work is done to examine the influence of the heated elliptical block on the thermal and dynamic structures in a square enclosure with moving top wall and cooled by the side walls. The calculations were performed for air (Pr = 0.71) as the operating fluid and a fixed value of Rayleigh number ($Ra = 10^4$). The Richardson number varies in the range 0.01 and 100 through the variations of Reynolds number $11.86 \leq Re \leq 1186.78$, as well as the position and orientation of the elliptical block are the control parameters in this work. The typical outcomes are illustrated in the form of current lines, isotherms and average Nusselt numbers and mean temperature.

Figure 4 presents the streamlines obtained for the heated elliptic cylinder block placed horizontally at X = 0.5 for different locations and various values of Richardson number. This later measures the importance of free convection caused by buoyancy forces and forced convection caused by lid-driven wall. For a dominating forced convection mechanism (Ri = 0.1), the streamlines in Figure 4a show that for Y = 0.25 the flow field is represented by a large cell that occupies the whole cavity and brings together the elliptical cylinder block. Consequently, the flow is mainly monocellular and rotates in a clockwise direction imposed by the kinematic condition given on the upper wall. Changing the position of the obstruction up to Y = 0.5 and 0.75, the flow structure remains unicellular but its intensity decreases. This decrease is justified by the fact that the cylinder block located close to the moving wall delays the flow. Also, the cell center is moved progressively closer to the right wall. For Ri = 1 (Figure 4b), the fluid flow is intensified by this increase in Ri for all positions of the cylinder block. In addition, in the lower left corner of the enclosure, a small trigonometric cell of very low intensity appears. The appearance of this cell is due to the increase in heat exchange by free convection in this area following the noticeable effect of buoyancy forces. Moreover, by climbing the obstacle at the top, this small cell changes relatively in size. The increase of Ri up to 10 (Figure 4c) results in an augmentation of the size and intensity of the small positive cell to the expense of the big one. Also, as the body moves upwards, the small cell undergoes slight changes in intensity.

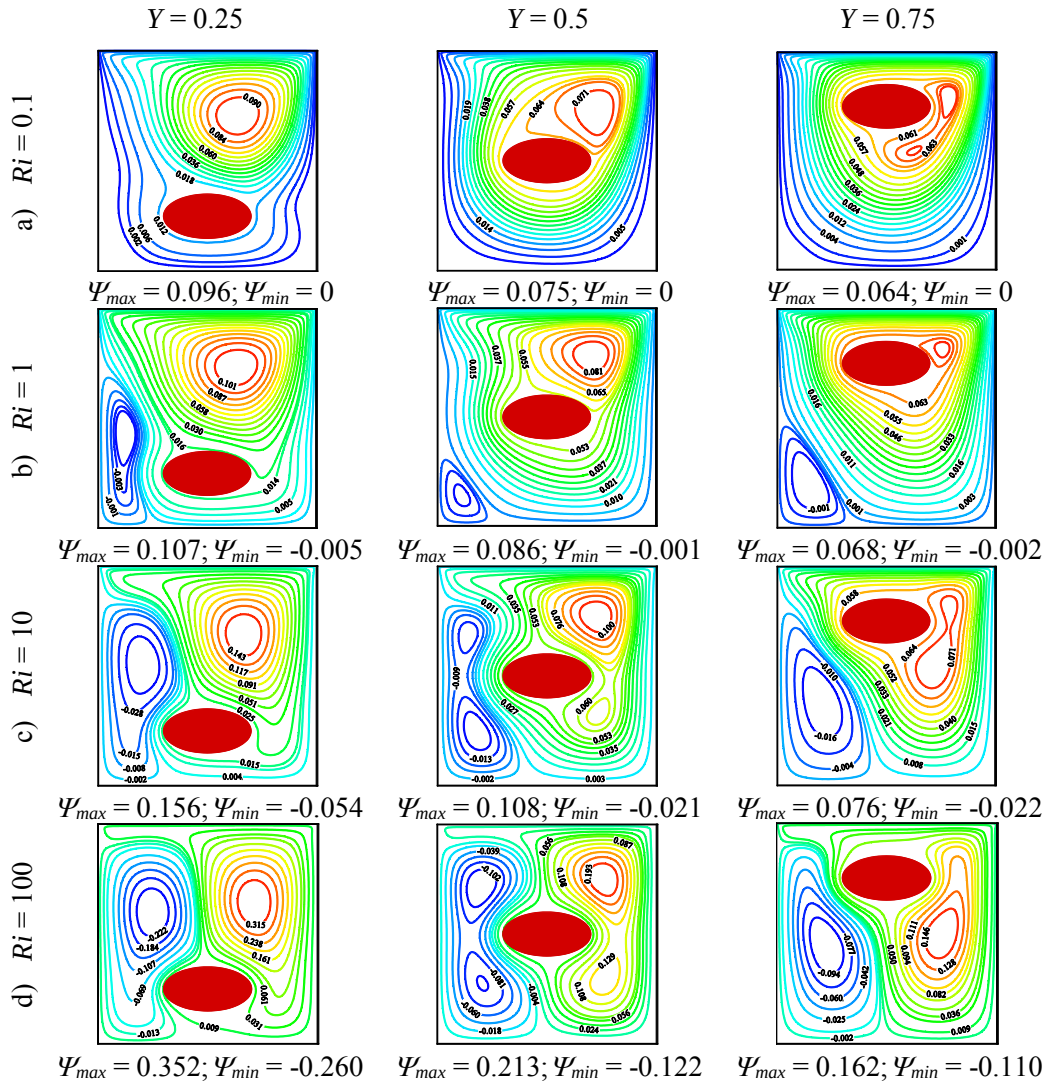

Fig. 4: Effect of horizontal cylinder block locations ($X = 0.5$) on the streamlines for various Richardson numbers Ri

For a large Richardson number value Ri = 100 the free convection regime dominates (Figure 4d), this increase in Ri indicates that the flow structure becomes bicellular characterized by two cells of the same shape and opposite direction and are driven by the buoyancy force for both cases of the elliptical cylinder placed close the top and lower walls of the enclosure, for the elliptical obstruction placed in the center of the enclosure, the dynamic structure is composed of four counter-rotating cells around the heated cylinder. It can also be seen that the vertical centerline of the cavity is an axis of symmetry of the flow structure. This symmetry is due to the symmetrical thermal limit conditions imposed and the importance of the flow velocity generated by the buoyancy forces in front of the velocity caused by the displacement of the upper wall.

The corresponding isotherms are illustrated in Figure 5 for the same parameters mentioned in Figure 4. It is observed from Figure 5a plotted for Ri = 0.1 that the isotherms are more condensed around the heated cylindrical block testifying in a good heat transfer between the heated block and the surrounding fluid. Also, the isotherms are parallel and constricted along the cold left vertical wall and at the top portion of the right one. This finding proves that the heat released by the block is evacuated to the outside through the vertical walls in these places. It is underlined that the movement of the block upwards involves homogenization of the temperature within the cavity. By increasing Richardson number progressively to 1 and 10, the temperature distribution remains qualitatively unchanged (Figure 5b and Figure 5c). Figure 5d shows that by raising the Richardson number from

10 to 100 (dominant natural convection), the isotherms become practically parallel to cold vertical walls and symmetrical about the vertical centerline. This increase in Ri shows that the increase in thickness of the boundary layer leads to a reduction in the temperature gradient near the vertical walls, i.e. a decrease in heat exchange between the cold walls and the fluid.

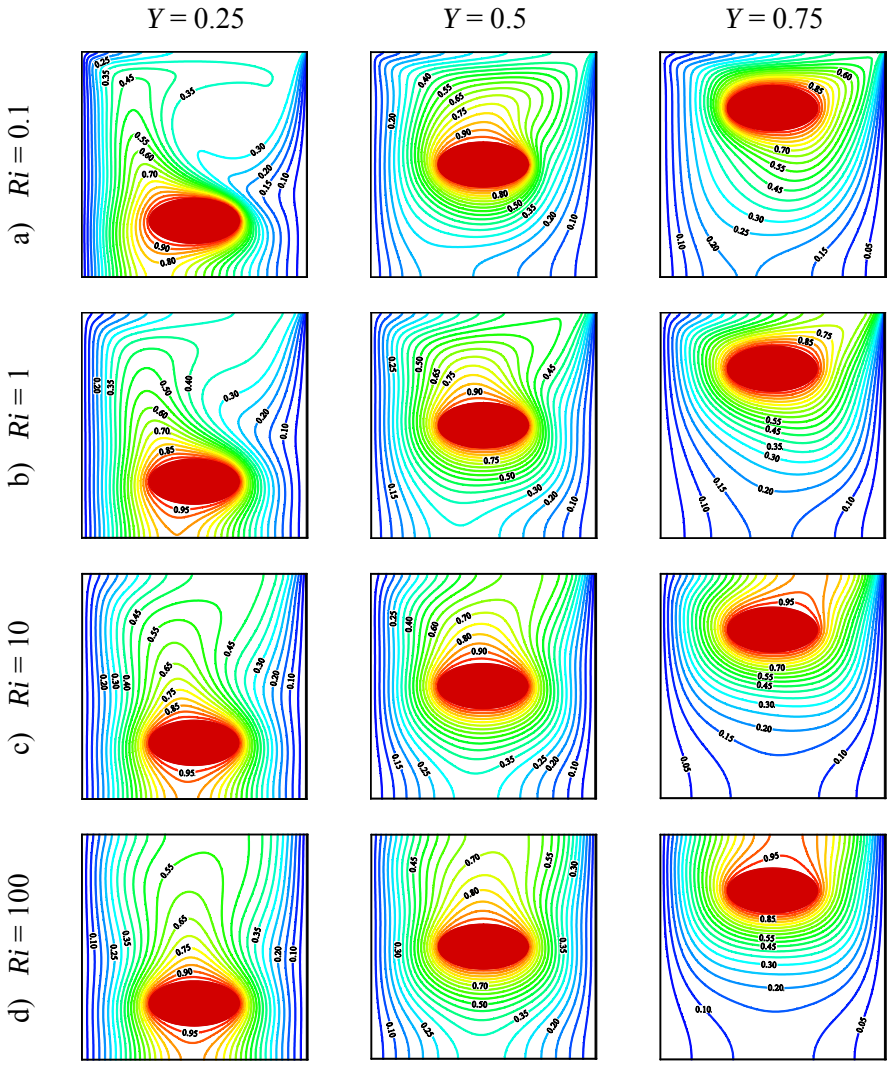

Fig. 5: Effect of horizontal cylinder block locations ($X = 0.5$) on the isotherms for several Richardson numbers Ri

Figure 6 presents the streamlines obtained for the hot elliptical block placed vertically at Y = 0.5 for three locations and various Richardson numbers. For Ri = 0.1 (Figure 6a) when the cylinder block is positioned near to the left wall, the streamlines show that the flow structure consists of a big cell, turning clockwise, containing the block and occupying almost the whole cavity. Another small positive cell forms in the lower right corner. When the block is localized in the center of the cavity, the flow is perfectly monocellular. It is indicated that the flow between the inner block and the rigid walls is similar to a flow in the channel. By changing the location of the block from the center to the right (X = 0.75), the dynamic structure is composed of the same large cell with the presence of a relatively trigonometric cell situated in the bottom left corner. These secondary cells, involved in the buoyancy forces, favor the natural convection heat transfer. In addition, we note that the large cell center shifts to the right wall following the displacement of the block.

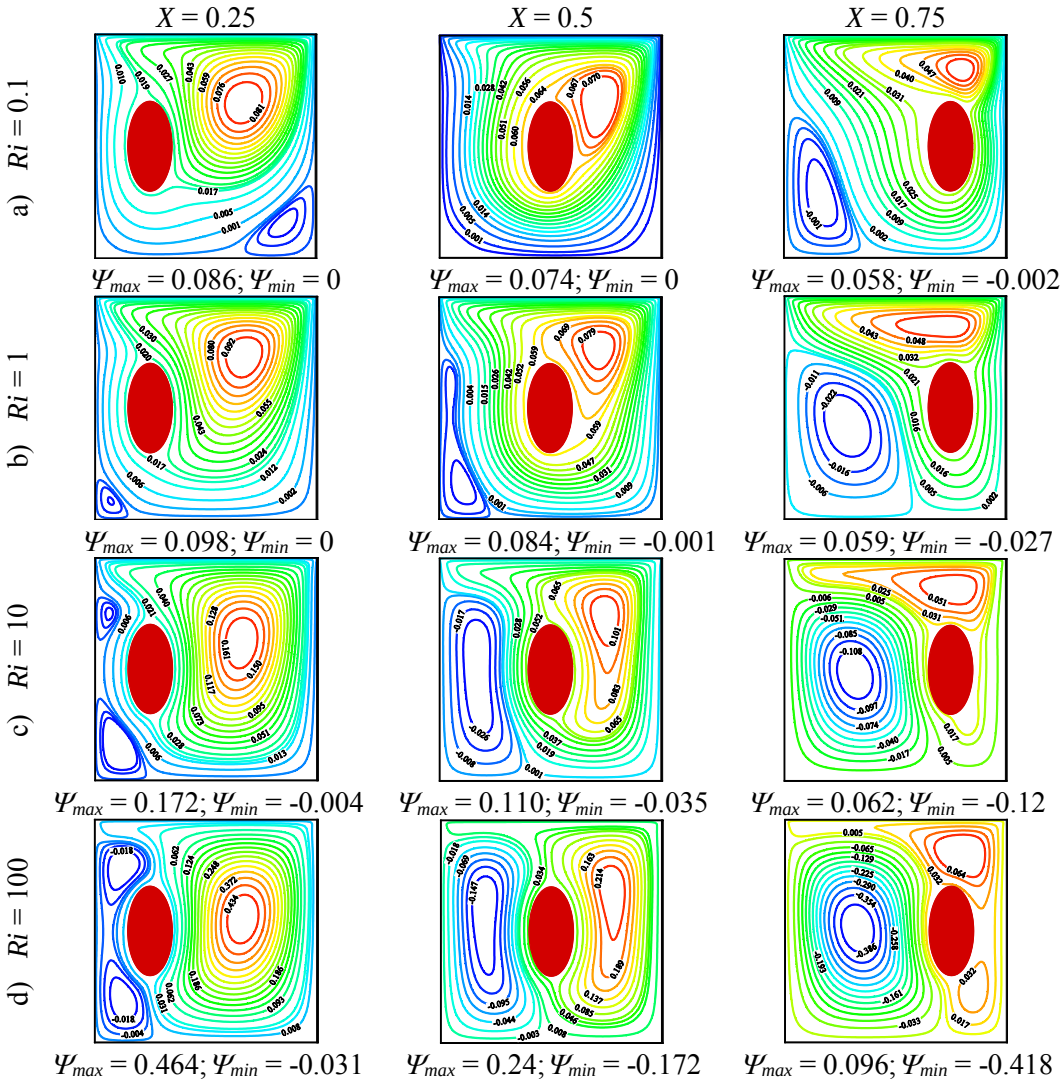

Fig. 6: Effect of vertical cylinder block locations at ($Y = 0.5$) on the streamlines for various Richardson numbers Ri

From the examination of the Figure 6b, Figure 6c and Figure 6d corresponding to Ri = 1, Ri = 10 and Ri = 100 respectively, we can see that the flow structure is intensified and a second convective cell has occurred close to the left vertical wall. The development in volume and intensity of this latter cell at the expense of the big cell is favored by X and Ri. More precisely, for X = 0.75 and Ri = 10, the second cell occupies almost the left half of the enclosure and consequently, the flow structure becomes bicellular. Finally, this change in the dynamic aspect of the flow causes a drastic change in the heat exchange rate and also determines the most dominant convection regime.

Figure 7 displays the isotherms corresponding to the streamlines presented in Figure 6. Generally, changing horizontally the position of the block from left to right of the cavity (increase of X) modifies the temperature distribution throughout the cavity and leads to its homogenization. On the contrary, the augmentation in Ri, i.e. decreases the speed of the upper wall and favors the natural heat exchange near the cold isothermal walls since the isotherms are condensed and layered near these latter walls.

Variations of the average Nusselt numbers $\overline{Nu}$, calculated on the cold walls according to the Richardson number Ri are illustrated in Figure 8 and Figure 9 for the case of the elliptical block placed horizontally (Figure 8) and vertically (Figure 9) and three locations for each orientation. It can be noted that, for all considered orientations and locations, $\overline{Nu}$ undergoes a drastic decrease, limited in the interval $0.01 \leq Ri \leq 1$, followed by asymptotic behavior in the remaining range of Ri. Such a result indicates that as the heat exchange by

natural convection is increasing, to the detriment of the forced one, as the mixed heat transfer rate decreases. For each orientation, the effect of block location on $\overline{Nu}$ is well noted. Indeed, heat transfer is very important by placing the block vertically close to the left wall (X = 0.25) or horizontally near the lower wall (Y = 0.25). In addition, from the analysis of the curves X = 0.5 and Y = 0.5 we can deduce that the horizontal orientation is better for heat transfer compared to the vertical case.

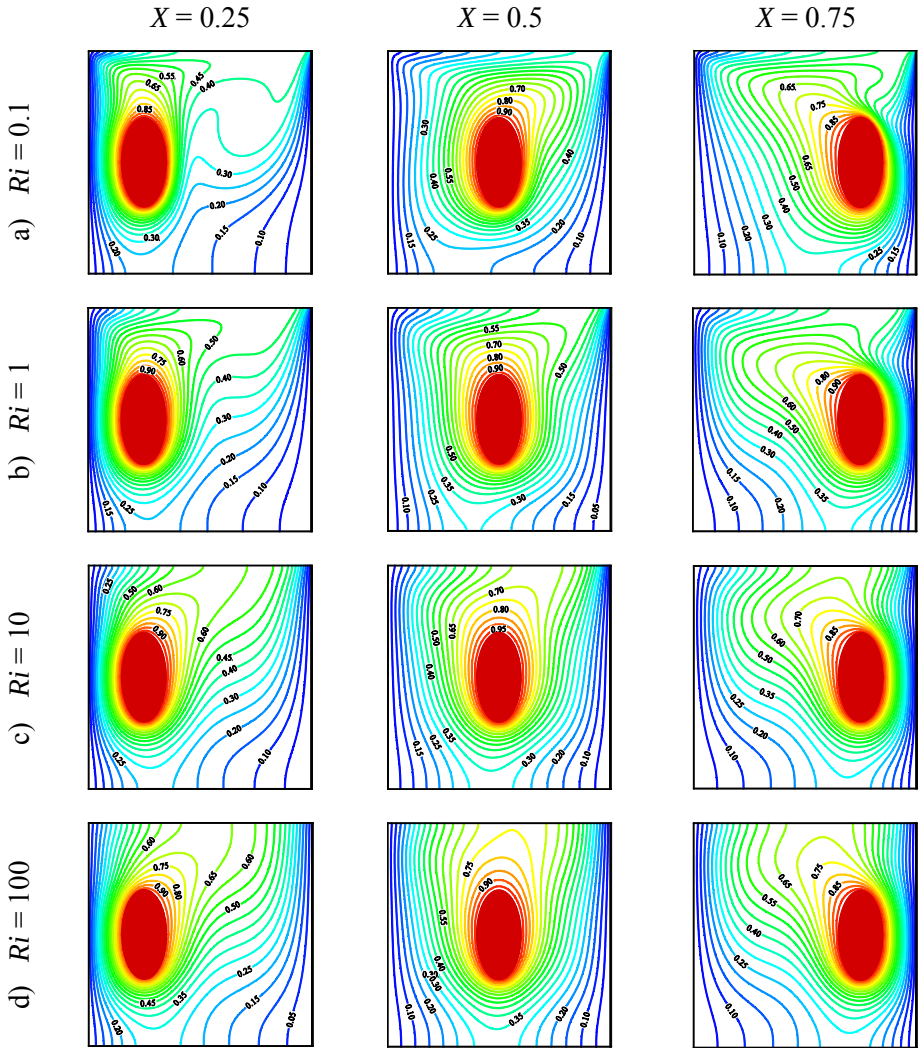

Fig. 7: Effect of vertical cylinder block locations ($Y = 0.5$) on the isotherms for several Richardson numbers *Ri*

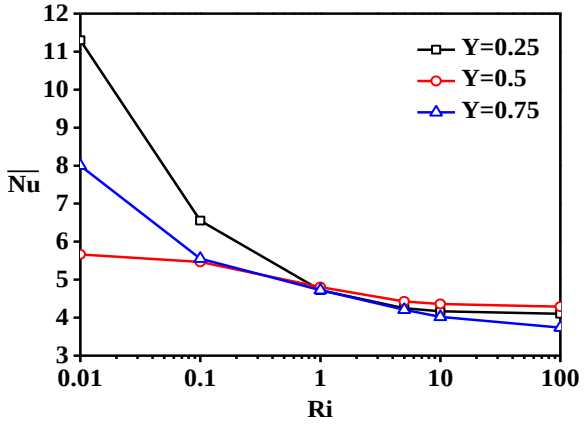

Fig. 8: Variations of the average Nusselt number vs. Ri for various cylinder locations for a horizontal elliptical block at X = 0.5

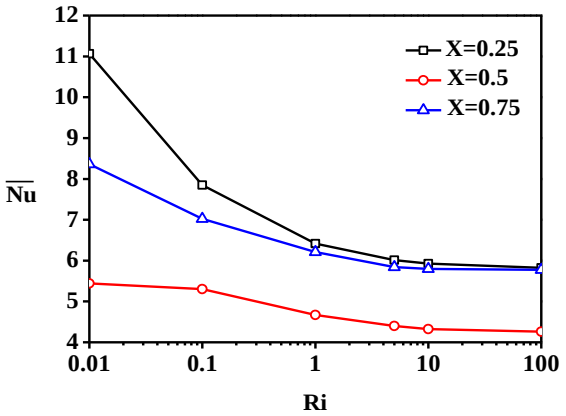

Fig. 9: Variations of the average Nusselt number vs. Ri for various locations of the cylinder for vertical elliptic block at Y = 0.5.

The calculation of the fluid's mean temperature inside the cavity is crucial for practical purposes. For this reason, the fluid's average temperature contained within the cavity is presented in Figure 10 and Figure 11 for horizontal and vertical elliptic blocks, respectively, and for different positions of the elliptic block. Figure 10 demonstrates that the fluid's average temperature contained within the cavity is characterized by a significant decrease for both positions Y = 0.25 and Y = 0.75 and for low values of the Richardson number Ri ≤ 0.1 (forced convection dominates). By increasing Ri, the mean temperature remains almost constant for the case where the elliptical block is located close to the upper wall Y = 0.75, on the other hand, for the case where the block is positioned close to the lower surface Y = 0.25, the average temperature is characterized by a minimum at Ri = 0.15. The evolution of the fluid's average temperature contained within the cavity is indicated by a continuous monotonic increase according to the Richardson number when the elliptical cylinder block is placed at the cavity center Y = 0.5. As a result, it can be seen from this figure that the position of the cylinder near the top wall (Y = 0.75) leads to a better overall cooling of the enclosure since the values of the $\bar{T}$ are lower compared to the other positions for Ri ≤ 0.1. For the case where the elliptical block is vertically oriented, the variation of the mean temperature of the fluid $\bar{T}$ versus Ri and for various block locations is shown in Figure 11. It can be seen that the mean temperature follows almost the same trend as that for the horizontal block and all positions, with a clear decrease and the minimum observed becomes large for X = 0.25 compared to Y = 0.25 in the horizontal case. As a conclusion of this figure, the cavity is cooler for the cases where the elliptical cylinder is positioned vertically close to the left cold wall and in the cavity center for Ri = 0.15 and Ri = 0.01, respectively.

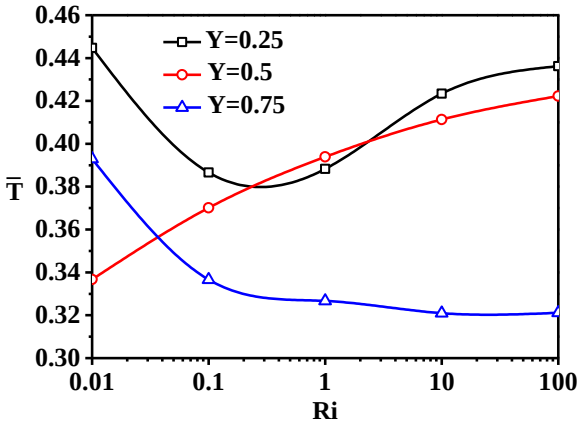

Fig. 10: Variation of mean fluid temperature vs. Richardson number for various positions of horizontal elliptic block at X = 0.5.

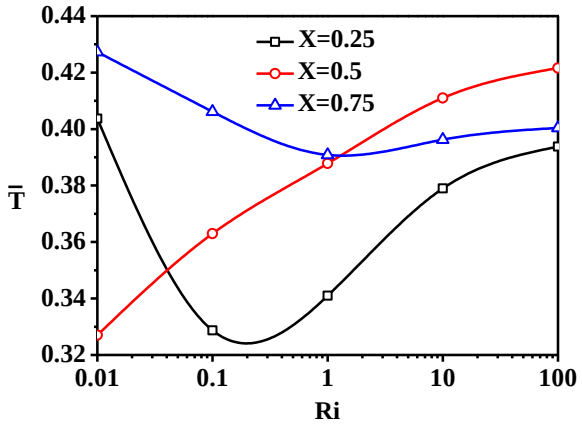

Fig. 11: Variation of mean fluid temperature vs. Richardson number for various positions of vertical elliptic block at Y = 0.5.

5 Conclusions

The problem of combined forced and free convection inside a square enclosure with a moving wall, containing a hot elliptical cylinder full of air is investigated numerically using the Lattice Boltzmann method. The enclosure is cooled from its sides by a cold temperature, whereas the remaining walls of the enclosure are considered thermally insulated. The mixed convection impact is attained by the heating elliptic block and moving upper wall. The combined effects of orientation and location of the block and Richardson number on heat transfer and flow behavior are examined. From the results presented, several interesting conclusions can be derived.

- The temperature distribution and flow structure are very responsive to geometrical parameters

such as the location of the elliptical cylinder (block) and flow parameters, especially Ri.

- It is found that the heat exchange rate can be enhanced by moving horizontally /(vertically) elliptical cylinder (block) to the left wall, (0.25;0.5) / (the lower wall, (0.5;0.25)).
- The heat transfer is very important for a horizontal elliptical cylinder (block) position in comparison with a vertical one for the different locations.
- The geometric configuration where the elliptical cylinder (block) is placed horizontally near to the top wall (0.5;0.75) leads to an improved cooling of the enclosure for Ri ≥ 1.
- For Ri = 0.01, by moving the vertical block from the center towards the vicinity of the left/ (the right) wall, the heat transfer rate increases from 5.44 to 11.06/(8.36) with an increase of 103.30%/(53.67%).

This research offers a thorough insight into the thermal and dynamic behavior of the system and showcases the Lattice Boltzmann Method's efficacy in studying heat transfer within a cavity featuring an elliptical block. Looking ahead, future inquiries should encompass the exploration of non-uniform dynamic and thermal boundary conditions on the cavity's walls. Diversifying the geometries of internal obstacles will contribute valuable insights into their effects on fluid dynamics and heat transfer.

Nomenclature

c	Lattice speed, $c = 1$
$\vec{c}_k$	Discrete vector velocity
c_s	Sound speed (m/s)
$D2Q9$	Lattice arrangement
f_k	Dynamical distribution function
f_k^{eq}	Equilibrium dynamical function
F_k	Direction of the imposed body force
g	Gravitational acceleration (m/s^2)
g_k	Thermal distribution function
g_k^{eq}	Equilibrium thermal function
Gr	Grashof number
L	Length of the cavity (m)
LBM	Lattice Boltzmann Method
Nu	Local Nusselt number
$\overline{Nu}$	Average Nusselt number
p	Dimensional pressure (Pa)
P	Dimensionless pressure
Pr	Prandtl number
Re	Reynolds number
Ri	Richardson number
t	Dimensionless time
t'	Dimensional time (s)
T_m	Dimensionless reference temperature
T'	Dimensional temperature (K)
T	Dimensionless temperature
(u, v)	Dimensional velocity components (m/s)
(U, V)	Dimensionless velocity components
u_0	Velocity lid-driven (m/s)
(x, y)	Dimensional coordinates
(X, Y)	Dimensionless coordinates

Greek symbols

α	Thermal diffusivity (m^2/s)
β	Thermal expansion coefficient (1/K)
$\Delta t'$	Time step (s)
$\Delta T'$	Dimensional temperature difference (K)
ρ	Density (Kg/m^3)
τ_f	Hydrodynamic relaxation time (s)
τ_g	Thermal relaxation time (s)
ϑ	Kinematic viscosity (m^2/s)
Ψ	Dimensionless stream function
ω_k	Weighting factor

Subscripts

C	Cold temperature
H	Hot temperature
max	Maximum
min	Minimum

Superscripts

$'$	Dimensional variable

References:

[1] Hidki, R., El Moutaouakil, L., Boukendil, M., Charqui, Z., Zrikem, Z., Abdelbaki, A., Mixed convection and surface radiation in a ventilated cavity containing two heat-generating solid bodies, *Materials Today: Proceedings*, Vol.66, 2022, pp. 318-324.

[2] Ben Abdelmlek, K., Ben Nejma, F., Energy Efficiency Analysis of Natural Convection Heat Transfer in Concentric Annulus with Interior and Exterior Grooves, *WSEAS Transactions on Heat and Mass Transfer*, vol. 18, 2023, pp. 99-118, https://doi.org/10.37394/232012.2023.18.10.

[3] Munshi, M. J. H., Alim, M. A., Bhuiyan, A. H., Ali, M., Hydrodynamic mixed convection in a lid-driven square cavity including elliptic shape heated block with corner heater, *Procedia engineering*, Vol.194, 2017, pp. 442-449.

[4] Kalteh, M., Javaherdeh, K., & Azarbarzin, T., Numerical solution of nanofluid mixed convection heat transfer in a lid-driven square cavity with a triangular heat

source, *Powder Technology*, Vol.253, 2014, pp. 780-788.

[5] Keya, S. T., Yeasmin, S., Rahman, M. M., Karim, M. F., Amin, M. R., Mixed convection heat transfer in a lid-driven enclosure with a double-pipe heat exchanger, *International Journal of thermofluids*, Vol.13, 2022, pp. 100131.

[6] Sereir, T., Missoum, A., Mebarki, B., Elmir, M., Mohamed, D., Optimal Conditions of Natural and Mixed Convection in a Vented Rectangular Cavity with a Sinusoidal Heated Wall Inside with a Heated Solid Block, *WSEAS Transactions on Heat and Mass Transfer*, vol. 15, 2020, pp. 195-208, https://doi.org/10.37394/232012.2020.15.23.

[7] Souai, S., Trabelsi, S., Sediki, E, LBM simulation for combined thermal radiation and natural convection in 2D enclosure with multiple solid blocks, *Numerical Heat Transfer, Part A: Applications*, 2023, pp. 1-26.

[8] Benderradji, R., Brahimi, M., Khalfallah, F., Numerical Study of Heat Transfer by Mixed Convection in a Cavity Filled with Nanofluid: Influence of Reynolds and Grashof Numbers, *International Journal of Applied Mathematics, Computational Science and Systems Engineering*, vol. 4, 2022, pp. 77-86.

[9] Daiz, A., Bahlaoui, A., Arroub, I., Belhouideg, S., Raji, A., Hasnaoui, M., Analysis of Mixed Convection in a Lid-driven Cavity with an Inner Hot Elliptical Block: Effect of Block Inclination, *Computational Thermal Sciences an International Journal*, Vol.16, 2024, pp. 1-23.

[10] Daiz, A., Bahlaoui, A., Arroub, I., Belhouideg, S., Raji, A., Hasnaoui, M., Modeling of nanofluid mixed convection within discretely heated lid-driven inclined cavity using lattice Boltzmann method, *AIP Conference Proceedings*, Vol.2761, 2023, pp. 040018.

[11] Arroub, I., Bahlaoui, A., Raji, A., Hasnaoui, M., Naïmi, M., Varying heating effect on mixed convection of nanofluids in a vented horizontal cavity with injection or suction, *Heat Transfer Engineering*, Vol.40, 2019, pp. 941-958.

[12] Altaee, A. H., Ali, F. H., Mahdi, Q. A., Natural convection inside square enclosure containing equilateral triangle with different orientations, *Journal of University of Babylon*, Vol.25, No.4, 2017, pp. 1194-1205.

[13] Olayemi, O. A., Khaled, A. F., Temitope, O. J., Victor, O. O., Odetunde, C. B., Adegun, I. K., Parametric study of natural convection heat transfer from an inclined rectangular cylinder embedded in a square enclosure, *Australian Journal of Mechanical Engineering*, Vol.21, No.2, 2021, pp. 1-14.

[14] Bararnia, H., Soleimani, S., Ganji, D. D., Lattice Boltzmann simulation of natural convection around a horizontal elliptic cylinder inside a square enclosure, *International Communications in Heat and Mass Transfer*, Vol.38, 2011, pp. 1436-1442.

[15] Adegun, I. K., Ibitoye, S. E., Bala, A., Effect of selected geometric parameters on natural convection in concentric square annulus, *Australian Journal of Mechanical Engineering*, Vol.20, No.4, 2022, pp. 1142-1153.

[16] Mansour, M. A., Gorla, R. S. R., Siddiqa, S., Rashad, A. M., Salah, T., Unsteady MHD natural convection flow of a nanofluid inside an inclined square cavity containing a heated circular obstacle, *International Journal of Nonlinear Sciences and Numerical Simulation*, Vol.24, 2021, pp. 000010151520200138.

[17] Moussaoui, M. A., Lahmer, E. B., Admi, Y., Mezrhab, A., Natural convection heat transfer in a square enclosure with an inside hot block, *Int. Conf. Wireless Technologies, Embedded and Intelligent Sys*tems, 2019, pp. 1-6.

[18] Chowdhury, K., Alim, A., Hossen, M., Natural Convection in a Partially Heated and Cooled Square Enclosure Containing a Diamond Shaped Heated Block, *International Journal of Fluid Mechanics and Thermal Sciences*, Vol.6, No.1, 2020, pp. 1-8.

[19] Hossain, M. S., Fayz-Al-Asad, M., Mallik, M. S. I., Yavuz, M., Alim, M. A., Khairul Basher, K. M., Numerical Study of the Effect of a Heated Cylinder on Natural Convection in a Square Cavity in the Presence of a Magnetic Field, *Mathematical and Computational Applications*, Vol.27, No.4, 2022, pp. 58.

[20] Parthasarathy, R. K., Mahadevan, S., Marimuthu, U., Numerical investigation of forced convection conjugate heat transfer from offset square cylinders placed in a confined channel covered by solid wall, *Heat*

Transfer—Asian Research, Vol.46, No.2, 2017, pp. 91-110.

[21] Admi, Y., Moussaoui, M. A., Mezrhab, A., Numerical Investigation of Convective Heat Transfer and Fluid Flow Past a Three-Square Cylinders Controlled by a Partition in Channel, *International Journal of Renewable Energy Development*, Vol.11, No.3, 2022, pp. 766-781.

[22] Prajapati, Y. K., Influence of fin height on heat transfer and fluid flow characteristics of rectangular microchannel heat sink, *International Journal of Heat and Mass Transfer*, Vol.137, 2019, pp. 1041-1052.

[23] Roy, K., Giri, A., Singh, M. R., Experimental Investigation of Forced Convective Cooling of Rectangular Blocks, *In Advances in Mechanical Engineering, Springer*, 2020, pp. 687-697.

[24] Lahmer, E. B., Admi, Y., Moussaoui, M. A., Mezrhab, A., Improvement of the heat transfer quality by air cooling of three-heated obstacles in a horizontal channel using the lattice Boltzmann method, *Heat Transfer*, Vol.51, 2022, pp. 3869-3891.

[25] Chamkha, A. J., Hussain, S. H., Abd-Amer, Q. R., Mixed convection heat transfer of air inside a square vented cavity with a heated horizontal square cylinder, *Numerical Heat Transfer, Part A: Applications*, Vol.59, No.1, 2011, pp. 58-79.

[26] Rahman, M. M., Parvin, S., Hasanuzzaman, M., Saidur, R., Rahim, N. A., Effect of heat-generating solid body on mixed convection flow in a ventilated cavity, *Heat transfer engineering*, Vol.34, no.15, 2013, 1249-1261.

[27] Gupta, S. K., Chatterjee, D., Mondal, B., Investigation of mixed convection in a ventilated cavity in the presence of a heat conducting circular cylinder, *Numerical Heat Transfer, Part A: Applications*, Vol.67, 2015, pp. 52-74.

[28] Islam, A. W., Sharif, M. A., Carlson, E. S., Mixed convection in a lid-driven square cavity with an isothermally heated square blockage inside, *International Journal of Heat and Mass Transfer*, Vol.55, 2012, pp. 5244-5255.

[29] Khanafer, K., Aithal, S. M., Laminar mixed convection flow and heat transfer characteristics in a lid-driven cavity with a circular cylinder, *International Journal of Heat and Mass Transfer*, Vol.66, 2013, pp. 200-209.

[30] Zheng, G. F., Ha, M. Y., Yoon, H. S., Park, Y. G., A numerical study on mixed convection in a lid-driven cavity with a circular cylinder, *Journal of Mechanical Science and Technology*, Vol.27, 2013, pp. 273-286.

[31] Biswas, N., Manna, N. K., Mahapatra, P. S., Enhanced thermal energy transport using adiabatic block inside lid-driven cavity, *International Journal of Heat and Mass Transfer*, Vol.100, 2016, pp. 407-427.

[32] Gangawane, K. M., Oztop, H. F., Ali, M. E., Mixed convection in a lid-driven cavity containing triangular block with constant heat flux: Effect of location of block, *International Journal of Mechanical Sciences*, Vol.152, 2019, pp. 492-511.

[33] Arroub, I., Bahlaoui, A., Raji, A., Hasnaoui, M., Naïmi, M., Cooling enhancement by nanofluid mixed convection inside a horizontal vented cavity submitted to sinusoidal heating, *Engineering Computations*, Vol.35, 2018, pp. 1747-1773.

[34] Ray, S., Chatterjee, D., MHD mixed convection in a lid-driven cavity including heat conducting circular solid object and corner heaters with Joule heating, *International Communications in Heat and Mass Transfer*, Vol.57, 2014, pp. 200-207.

[35] Mohamad, A. A., *Lattice Boltzmann Method*, Springer, 2011.

[36] Mezrhab, A., Moussaoui, M. A., Naji, H., Lattice Boltzmann simulation of surface radiation and natural convection in a square cavity with an inner cylinder, *Journal of Physics D: Applied Physics*, Vol.41, 2008, pp. 115502.

[37] Rosdzimin, A. R. M., NA Che Sidik, S. M. Zuhairi, Study of Plume Behaviour Two Heated Cylinders at High Rayleigh Number Using Lattice Boltzmann Method, *AIP Conference Proceedings*, Vol.1225, 2010, pp. 780-787.

[38] Mohebbi, R., Rashidi, M. M., Numerical simulation of natural convection heat transfer of a nanofluid in an L-shaped enclosure with a heating obstacle, *Journal of the Taiwan Institute of Chemical Engineers,* Vol.72, 2017, pp. 70-84.

[39] Karki, P., Yadav, A. K., Arumuga Perumal, D., Study of adiabatic obstacles on natural convection in a square cavity using lattice Boltzmann method, *Journal of Thermal*

Science and Engineering Applications, Vol.11, 2019, pp. 034502.

[40] Farrokhpanah, A., Nabovati, A., & Mostaghimi, J., Study of curved boundary treatments in lattice Boltzmann method, *In Proceedings of The Canadian Society for Mechanical Engineering International Congress*, 2014.

Contribution of Individual Authors to the Creation of a Scientific Article (Ghostwriting Policy)

The authors equally contributed to the present research, at all stages from the formulation of the problem to the final findings and solution.

Sources of Funding for Research Presented in a Scientific Article or Scientific Article Itself

No funding was received for conducting this study.

Conflict of Interest

The authors have no conflicts of interest to declare that are relevant to the content of this article.